Oncogene (2012) 31, 764–775
© 2012 Macmillan Publishers Limited All rights reserved 0950-9232/12
www.nature.com/onc

ORIGINAL ARTICLE

Regulation of ovarian cancer progression by microRNA-187 through targeting Disabled homolog-2

A Chao[1,7], C-Y Lin[1,7], Y-S Lee[2,3], C-L Tsai[1], P-C Wei[1,4], S Hsueh[5], T-I Wu[1], C-N Tsai[6], C-J Wang[1], A-S Chao[1], T-H Wang[1,2,4] and C-H Lai[1]

[1]*Department of Obstetrics and Gynecology, Chang Gung Memorial Hospital and Chang Gung University College of Medicine, Tao-Yuan, Taiwan;* [2]*Genomic Medicine Research Core Laboratory, Chang Gung Memorial Hospital, Gwei-Shan, Taiwan;* [3]*Department of Biotechnology, Ming-Chuan University, Tao-Yuan, Taiwan;* [4]*Graduate Institute of Biomedical Sciences, Chang Gung University, Gwei-Shan, Taiwan;* [5]*Department of Clinical Pathology, Chang Gung Memorial Hospital and Chang Gung University College of Medicine, Tao-Yuan, Taiwan and* [6]*Graduate Institute of Clinical Medical Sciences, Chang Gung University, Gwei-Shan, Taiwan*

MicroRNAs (miRNAs) play important roles in tumorigenesis by regulating oncogenes and tumor-suppressor genes. In this study, miR-187 and miR-200a were found to be expressed at higher levels in ovarian cancers than in benign tumors. In patients with ovarian cancer, however, higher levels of miR-187 and miR-200a expression were paradoxically associated with better OS and recurrence-free survival. Further, multivariate analysis showed that miR-187 served as an independent prognostic factor for patients with ovarian cancer ($n = 176$). Computational prediction and microarray results indicated that miR-187 directly targeted Disabled homolog-2 (Dab2), and luciferase reporter assays confirmed that the target site of miR-187 was located at the 3′-UTR of the Dab2 gene. Generally considered as a tumor-suppressor gene, Dab2 may actually promote tumor progression in advanced cancers through epithelial-to-mesenchymal transition (EMT). Ectopic expression of miR-187 in cancer cells promoted cell proliferation, but continued overexpression of miR-187 suppressed Dab2 and inhibited migration. Suppression of miR-187 upregulated Dab2, which, by inhibiting E-cadherin levels while stimulating vimentin and phospho-FAK levels, promoted EMT. Reduced ovarian cancer Dab2 histoscores correlated with high miR-187 levels and improved outcomes of patients. Collectively, these results demonstrate distinct dual roles of Dab2 in cell proliferation and tumor progression. In the initial steps of tumorigenesis, upregulated miR-187 suppresses Dab2, promoting cell proliferation. During the later stages, however, continued increased levels of miR-187 inhibits the Dab2-dependent EMT that is associated with tumor invasiveness, which is presumed to be the reason why cancers with high miR-187 levels were associated with better survivals.

Oncogene (2012) **31,** 764–775; doi:10.1038/onc.2011.269; published online 4 July 2011

Keywords: microRNA; miR-187; Dab2; epithelial–mesenchymal transition (EMT)

Introduction

Epithelial ovarian cancer is one of the deadliest malignancies in women (Jemal *et al*., 2007). The 5-year survival rate of ovarian cancer has remained relatively unchanged despite extensive efforts to improve the efficacy of treatment (Berek *et al*., 2010). Although CA-125 may be a valuable tool in the follow-up of metastasizing ovarian cancer (Bast *et al*., 1981), the poor prognosis of this malignancy emphasizes the need to improve disease detection and prognostic stratification.

MicroRNAs (miRNAs) are evolutionarily conserved, non-coding RNA molecules that are usually 21–25 nucleotides in length, which function by binding to the 3′-untranslated regions (3′-UTRs) of mRNAs, where they repress protein translation or promote mRNA degradation (Bartel, 2004; Griffiths-Jones, 2004). miRNAs are involved in processes as diverse as apoptosis, the cell cycle, angiogenesis and epithelial-to-mesenchymal transition (EMT) (Gregory *et al*., 2008; Singh and Settleman, 2010). In recent years, growing evidence suggests that miRNAs may have oncogenic potential, and aberrant miRNA expressions have been found in many human cancers (Metzler *et al*., 2004; Takamizawa *et al*., 2004; Volinia *et al*., 2006; Yanaihara *et al*., 2006). Previous ovarian cancer studies have attempted to identify an aberrant miRNA expression signature by using snap-frozen specimens (Iorio *et al*., 2007; Lu *et al*., 2007; Nam *et al*., 2008; Yang *et al*., 2008) or formalin-fixed, paraffin-embedded (FFPE) tissues (Eitan *et al*., 2009; Hu *et al*., 2009). Iorio *et al*. (2007) showed that four miRNAs (miR-200a, miR-200b, miR-200c and miR-141) were significantly upregulated in ovarian cancer tissues. Using miRNA microarray analysis, Nam *et al*. (2008) demonstrated that overexpression of miR-200 in snap-frozen samples was associated with poor patient prognosis. However, a recent study using a PCR-based platform for miRNA expression profiling of

Correspondence: Professor T-H Wang or C-H Lai, Department of Obstetrics and Gynecology, Chang Gung Memorial Hospital, 5 Fu-Hsing Street, Gwei-Shan, Tao-Yuan 333, Taiwan.
E-mail: knoxtn@cgmh.org.tw or sh46erry@ms6.hinet.net
[7]These authors contributed equally to this work.
Received 15 November 2010; revised and accepted 31 May 2011; published online 4 July 2011

FFPE tissues suggested that overexpression of miR-200a was associated with a better prognosis in patients with advanced ovarian cancer (Hu *et al*., 2009). Although there were obviously distinct differences in assay technologies and tissue sources (Hu *et al*., 2009), the exact cause of these discrepancies is unclear.

Dab2 (Disabled homolog-2; gene ID 1601) was first cloned as DOC-2 (differentially expressed in ovarian cancer), which was present in normal ovarian surface epithelial cells but absent in ovarian cancer cell lines (Mok *et al*., 1994). Dab2 was considered to be a tumor suppressor because it is absent in 85% of ovarian cancer (Fazili *et al*., 1999). More recently, Dab2 was found to be involved in EMT (Prunier and Howe, 2005; Chaudhury *et al*., 2010). EMT is a tumor evolutionary process, in which cancer cells acquire invasive and metastatic properties (Singh and Settleman, 2010).

In this study, we first identified that two miRNAs, miR-187 and miR-200a, were significantly overexpressed in ovarian cancer. Surprisingly, we also found that increased levels of miR-187 and miR-200a in ovarian cancer correlated with the better prognostic group. To solve this paradox, we dissected the mechanistic roles of miR-187 and its target Dab2, and revealed the distinct dual roles of Dab2 in cell proliferation and tumor progression.

Results

Overexpression of miR-187 and miR-200a in human ovarian cancer cells

Table 1 summarizes the significantly differential expression of miRNAs between eight human ovarian cancer cell lines (SKOV3, OVCAR-3, TOV-21G, TOV112D, OV-90, BR, MDAH2774, CAOV3) and two immortalized ovarian surface epithelial cell lines (IOSE-80PC and HOSE), among a panel of 157 miRNAs analyzed. We identified 15 miRNAs that were upregulated in ovarian cancer, and selected the top two miRNAs (miR-187 and miR-200a) for further analyses.

Table 1 Differentially expressed miRNAs between ovarian cancer cell lines and HOSE cell lines

miRNA	P-*value*	*Log ratio*
miR-200a	0.003	15.0
miR-187	0.012	7.5
miR-200b	0.016	12.1
miR-98	0.025	5.2
miR-106a	0.027	5.6
miR-138	0.032	5.5
miR-17-5p	0.032	5.7
miR-374	0.033	4.3
miR-182[a]	0.035	5.8
miR-200c	0.036	7.5
miR-107	0.038	5.2
miR-194	0.040	4.2
miR-151	0.044	4.4
miR-141	0.048	7.6
miR-182	0.049	5.9
miR-154	0.023	−5.2
miR-368	0.040	−5.5

Abbreviations: HOSE, human ovarian surface epithelial cell line; miRNA, microRNA.
[a]Antisense.

Confirmation of high miR-187 and miR-200a expression in human ovarian cancer tissues

The expression levels of miR-187 and miR-200a in FFPE ovarian cancer tissues ($n=176$) were significantly higher than those seen in benign ovarian tissues ($n=20$) (Figure 1a). Expression of miR-187 was 2.8-fold higher in ovarian cancer tissues than in benign ovarian tissues

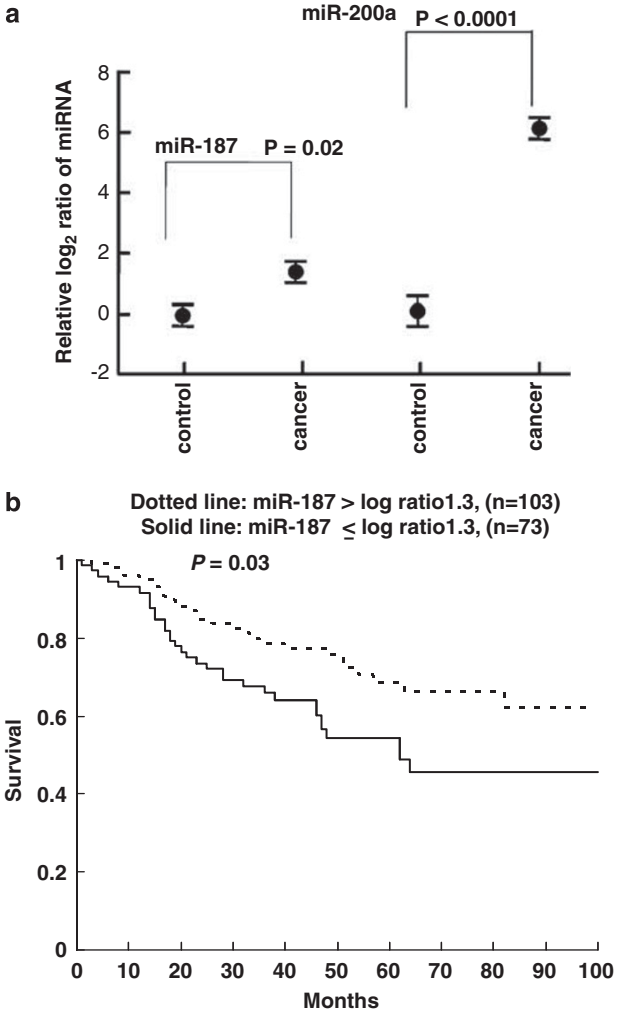

Figure 1 miR-187 and miR-200a were upregulated in ovarian cancer tissues, but cancers with poor prognosis were paradoxically associated with a lower miR-187 expression. (**a**) Real-time qPCR of miR-187 and miR-200a was performed on FFPE tissues of ovarian cancer (cancer, $n=176$) and benign ovarian tumors (control, $n=20$). The *y*-axis represents the $\log_2$ratio normalized by the value of the control. The results showed that the expression levels of miR-187 ($P=0.02$) and miR-200a ($P<0.0001$) were significantly upregulated in ovarian cancer tissues. The data are shown as the means ± s.e. (**b**) Kaplan–Meier OS curves analysis revealed that women with cancer expressing miR-187 ⩽log ratio 1.3 (solid line) had significantly ($P=0.03$) worse survivals than those with miR-187 >log ratio 1.3 (dotted line).

($P=0.02$), whereas the level of miR-200a expression was 74.5-fold higher ($P<0.0001$).

Prognostic value of miR-187 expression in patients with epithelial ovarian cancer

We sought to test the prognostic value of miR-187 and miR-200a levels in 176 patients with epithelial ovarian cancer. Their median follow-up time was 40 months (range: 3–109 months), and tumor histology included serous ($n=56$), mucinous ($n=28$), endometrioid ($n=52$) and clear cell ($n=40$) tumors (Supplementary Table 1). In univariate analyses, advanced stages III and IV, grade-3, and surprisingly, reduced expressions of miR-187 (log ratio $\leqslant 1.3$) or miR-200a (log ratio $\leqslant 5$) were significantly associated with a decreased overall survival (OS) (Supplementary Table 2). In multivariate analyses, lower levels of miR-187 ($P=0.019$) and advanced stages ($P<0.0001$) were the only significant, independent predictors for recurrence-free survival and OS (Table 2). Survival curve analyses also identified that low levels of miR-187 in ovarian cancer (log ratio $\leqslant 1.3$, $n=73$) were significantly associated with poorer prognosis than high levels of miR-187 (log ratio >1.3, $n=103$) (Figure 1b).

Dab2 was repressed by miR-187 in ovarian cancer cells

Dab2 is one of the genes targeted by miR-187, according to the TargetScan database (Figure 2a), and microarray analysis of gene expression showed that gene expressions of Dab2 were2.5-fold lower in ovarian cancer cell lines than in immortalized ovarian surface epithelial cells ($P<0.003$). To confirm that miR-187 directly suppressed Dab2 expression through the target sequences of the 3′-UTR of Dab2 mRNA, we constructed a pMir luciferase reporter vector (Luc-Dab2-3′-UTR) with the putative 3′-UTR target site for miR-187 located downstream from the luciferase gene. Co-transfected miR-187 significantly decreased the reporter activity of Luc-Dab2-3′-UTR, but did not affect the reporter activity of mut-Luc-Dab2-3′-UTR (Figure 2b). To support the inhibitory role of miR-187 on Dab2, transfection of anti-miR-187 significantly increased the reporter activity of Luc-Dab2-3′-UTR (Figure 2b).

To validate the suppressor role of miR-187 on endogenous Dab2, at both mRNA and protein levels, we compared the effects of miR-187, anti-miR-187 and scrambled control sequences in ovarian cancer cells. Transient overexpression of miR-187 in SKOV3 cells significantly inhibited endogenous Dab2 mRNA, whereas overexpression of anti-miR-187 significantly upregulated Dab2 (Figure 2c). Similar results were seen in protein regulation; overexpression of miR-187 suppressed endogenous Dab2 protein, whereas anti-miR-187 increased it (Figure 2d). The inhibitory effect of miR-187 on Dab2 protein levels was confirmed in other ovarian cancer cell lines. Transient overexpression of miR-187 significantly suppressed endogenous Dab2 protein levels in TOV112D cells that have a weak endogenous miR-187 expression, whereas transient transfection of anti-miR-187 significantly increased Dab2 proteins in OV90 cells that exhibit strong endogenous miR-187 expression (Supplementary Figure 1).

Effect of miR-187 on cell proliferation

Ectopic expression of miR-187 in SKOV3 cells suppressed Dab2 (Figure 2) and stimulated cell proliferation, as shown by increased bromodeoxyuridine (BrdU) incorporation (Figure 3a), compatible with the role of Dab2 as a tumor suppressor (Fazili *et al*., 1999). On the other hand, expression of anti-miR-187 inhibited BrdU incorporation (Figure 3d).

Invasiveness of ovarian cancer is regulated by the miR-187-targeted, DAB2-mediated induction of EMT

To solve the paradox as to why mildly increased levels of miR-187 in ovarian cancer were surprisingly associated with poorer prognoses for patients (Table 2), we examined the effect of miR-187 on regulation of cell migration. In transwell migration assays, overexpressed

Table 2 Multivariate analyses of clinicopathological covariates with miR-187 and miR-200a on RFS and OS ($n=176$)

Patient and tumor characteristics	*RFS hazard ratio (95% CI)*	P-*value*	*OS hazard ratio (95% CI)*	P-*value*
miR-187		**0.028**		**0.019**
Log ratio $\leqslant 1.3$	1.676 (1.058–2.654)		1.919 (1.116–3.301)	
Log ratio >1.3	1		1 (ref.)	
miR-200a		0.491		0.229
Log ratio $\leqslant 5.0$	1.213 (0.70–2.101)		1.466 (0.786–2.734)	
Log ratio >5.0	1		1 (ref.)	
Stage		**<0.0001**		**<0.0001**
I–II	0.174 (0.101–0.301)		0.150 (0.077–0.293)	
III–IV	1		1 (ref.)	
Grade		0.279		0.840
1, 2	0.683 (0.395–1.180)		0.936 (0.492–1.780)	
3	1		1 (ref.)	

Abbreviations: CI: confidence interval; OS: overall survival; RFS: recurrence-free survival.
Log ratio: miRNA expression level on $\log_2$ base in comparing with control.
The values of statistical significance are shown in bold.

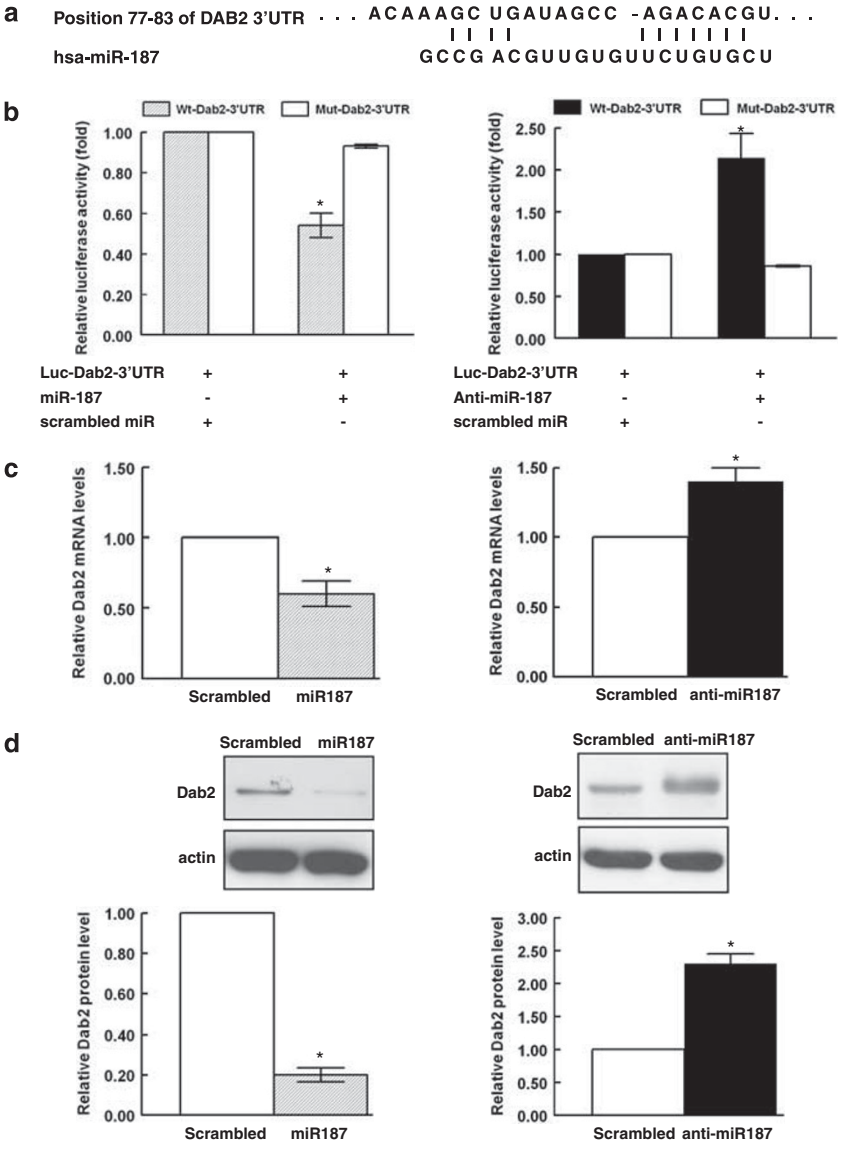

Figure 2 miR-187 targeted Dab2 in ovarian cancer. (**a**) A putative target site of miR-187 at the 3′-UTR of Dab2. (**b**) Effect of miR-187 on the luciferase activity of wild-type Luc-Dab2-3′-UTR (wt-Luc-Dab2-3′-UTR) and mut-Luc-Dab2-3′-UTR, in which two underlined nucleotides (ACAAAGCUGAUAGCCAGACAATU) were mutated. SKOV3 cells were transfected with Luc-Dab2-3′-UTR or mut-Luc-Dab2-3′-UTR along with miR-187, anti-miR-187 LNA oligonucleotide or a scrambled LNA oligonucleotide. Luciferase assays were performed 48 h and 72 h after transfection with miR-187 (left panel) and anti-miR-187 (right panel), respectively. The data are shown as the means ± s.e. of the relative luciferase activity, normalized to those of scrambled controls, from three independent experiments. $*P<0.05$ compared with controls. (**c**) Suppression of Dab2 mRNA by miR-187, as detected by real-time qPCR. Overexpression of miR-187 in the SKOV3 ovarian cancer cell line inhibited the mRNA expression of Dab2 (shaded bar). On the other hand, transfection with anti-miR-187 increases the mRNA expression of Dab2 (solid bar). A scrambled-sequence RNA was used as control. (**d**) miR-187 inhibited the protein level of Dab2, as analyzed by immunoblot relative to β-actin. Overexpression of miR-187 (shaded bar) in SKOV3 cells downregulated Dab2 protein levels. Suppression of endogenous miR-187 with anti-miR-187 (solid bar) increased Dab2 protein levels. Appropriate scrambled sequences (scrambled) were used as transfected controls. A representative western blot analysis using a mouse monoclonal antibody that recognized Dab2 (band at 96 kDa) is shown (upper panels). The shown as mean ± s.e. were derived from three independent experiments. $*P<0.05$ when compared with controls.

miR-187 suppressed Dab2 (Figure 2 and Supplementary Figure 2) and inhibited cell migration (Figure 3b), and expression of anti-miR-187 increased Dab2 protein levels (Figure 2 and Supplementary Figure 2) and stimulated cell migration (Figure 3e). In wound-closure assays, overexpression of miR-187 significantly suppressed cell migration (Figure 3c and Supplementary Figure 3a), whereas transfection with anti-miR-187 stimulated cell migration (Figure 3f and Supplementary Figure 3b). Furthermore, overexpression of miR-187 increased E-cadherin protein levels but decreased vimentin and phospho-focal adhesion kinase (phospho-FAK) protein levels, whereas transfection with anti-miR-187 exerted opposite effects (Figures 3g and h). Overexpression of miR-187 also changed ovarian cancer cells to a polygonal shape in addition

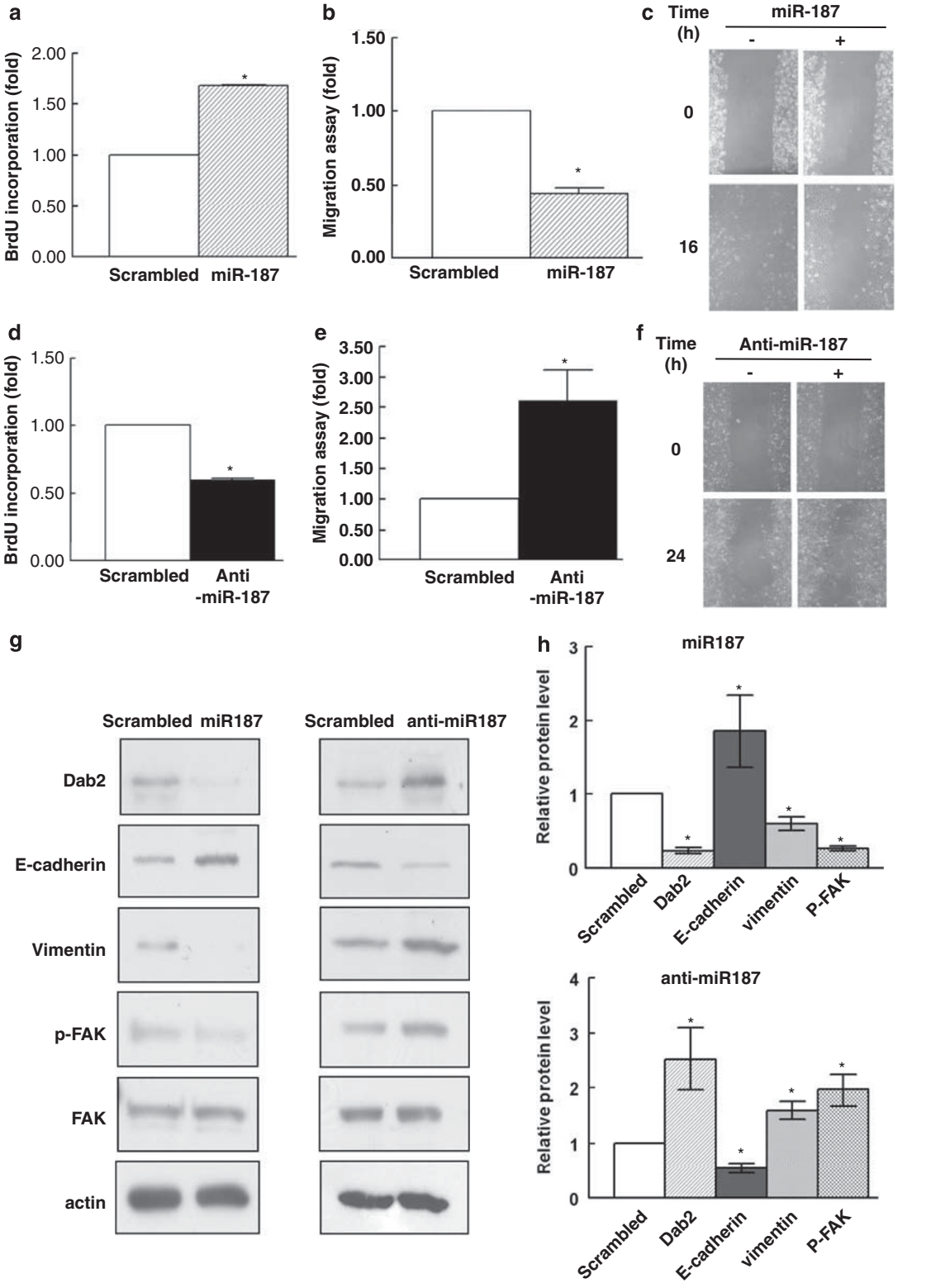

Figure 3 miR-187 promoted cell proliferation but inhibited EMT and cell migration by suppression of Dab2. Ectopic expression of miR-187 in SKOV3 cells promoted cell proliferation as assessed by the BrdU incorporation assays (**a**), but inhibited cell migration as analyzed by transwell migration assays (**b**) and wound-closure assays (**c**). Transfection with anti-miR-187 in SKOV3 cells exerted exactly opposite effects (**d**–**f**). The quantitative results of wound-closure assays are summarized in Supplementary Figures 3a and b. (**g**) Overexpression of miR-187 in SKOV3 cells suppressed Dab2, increased E-cadherin, and suppressed vimentin and phospho-FAK protein levels. By contrast, expression of anti-miR-187 increased Dab2, suppressed E-cadherin, and increased vimentin and phospho-FAK protein levels. Actin and total FAK were used to confirm equal protein inputs in all lanes. (**h**) Quantitative summary of the results shown in panel **g**. The data shown as mean ± s.e. are calculated from three independent experiments. $*P<0.05$ when compared with controls.

to decreased vimentin protein levels, whereas transfection with anti-miR-187 changed cancer cells back to a spindle-like mesenchymal cell shape with increased vimentin expression (Supplementary Figure 4a).

Reconstitution of Dab2 proteins overrode the effects of miR-187 on stimulation of cell proliferation (Figure 4a) and inhibition of cell migration (Figure 4b and Supplementary Figure 3c), and reversed the morphology and vimentin levels in SKOV3 ovarian cancer cells (Supplementary Figure 4b). Collectively, these results indicated that overexpression of miR-187 inhibited cell migration through inhibition of EMT. Inhibition of EMT by overexpression of miR-187 was mediated by suppression of Dab2, because reconstitution of Dab2 proteins rescued EMT (Figures 4c and d). Overexpression of Dab2 with the above reconstituting expression vector alone inhibited cell proliferation, stimulated cell migration and promoted EMT (Supplementary Figure 5).

Reverse correlations between miR-187 and Dab2 levels in clinical specimens

Reverse correlations between miR-187 levels and Dab2 protein levels, as well as those between miR-187 levels and Dab2 mRNA levels, were validated by immunohistochemical studies of human ovarian cancer FFPE tissues (Figure 5) and real-time quantitative PCR (qPCR) of fresh-frozen samples (Supplementary Figure 6), respectively. Dab2 protein expression was minimal in ovarian cancer cells with high miR-187 levels (Figure 5a), whereas ovarian cancer with low miR-187 levels had higher levels of Dab2 protein (Figure 5b). Benign ovarian tumors were used as positive controls for heavy Dab2 staining (Figure 5c). The histoscores of the group with low miR-187 expression (log ratio $\leqslant 1.3$, $n=73$) were significantly higher than the group with higher miR-187 expression (log ratio >1.3, $n=103$) (Figure 5d). In additional fresh-frozen ovarian cancer tissues ($n=20$), Dab2 RNA levels were also correlated negatively with miR-187 levels ($P=0.025$) (Supplementary Figure 6).

The effects of miR-187 on ovarian cancer cells were independent of miR-200a

To minimize the confounding effect of miR-200a on the miR-187–Dab2 regulatory system, we studied the effects of miR-187 in miR-200a-knockdown SKOV3 cells. In miR-200a-knockeddown cancer cells, overexpression of miR-187 inhibited Dab2 protein levels, increased cell proliferation (Figure 6a) and inhibited EMT, which was

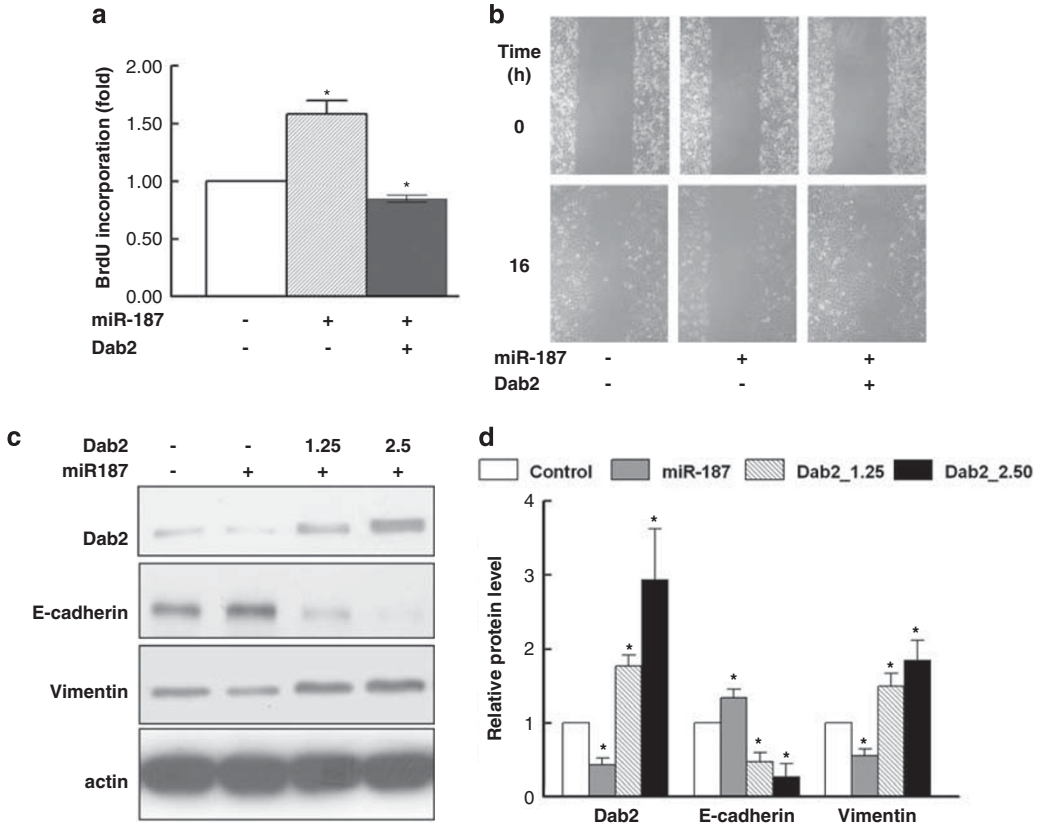

Figure 4 Effects of miR-187 were overridden by reconstitution of T7-tagged Dab2, which was not suppressed by miR-187. (**a**) Increased cell proliferation induced by miR-187 was significantly inhibited when the cells were reconstituted with Dab2. (**b**) Inhibition of cell migration induced by miR-187 was abolished by reconstitution with Dab2. The quantitative results of wound-closure assays are summarized in Supplementary Figure 3c. (**c**) In a dose-dependent manner, reconstitution of Dab2 decreased E-cadherin and increased vimentin, rescuing Dab2-mediated EMT. (**d**) A quantitative summary of Dab2, E-cadherin and vimentin protein levels. The data shown as mean ± s.e. are calculated from three independent experiments. $*P<0.05$ when compared with controls.

shown by increased E-cadherin protein and decreased vimentin levels (Figure 6c and Supplementary Figure 7a). In the same miR-200a-knockdown cancer cells, transfection with anti-miR-187 exerted the opposite effects of miR-187 (Figures 6b and d, and Supplementary Figure 7b). ZEB1 is a known target gene of miR-200a. In those experiments, knockdown of miR-200a was confirmed by increased levels ZEB1 (Supplementary Figures 8a and b) and by increased activities of the Luc-ZEB1-3′-UTR reporter (Supplementary Figures 8c and d).

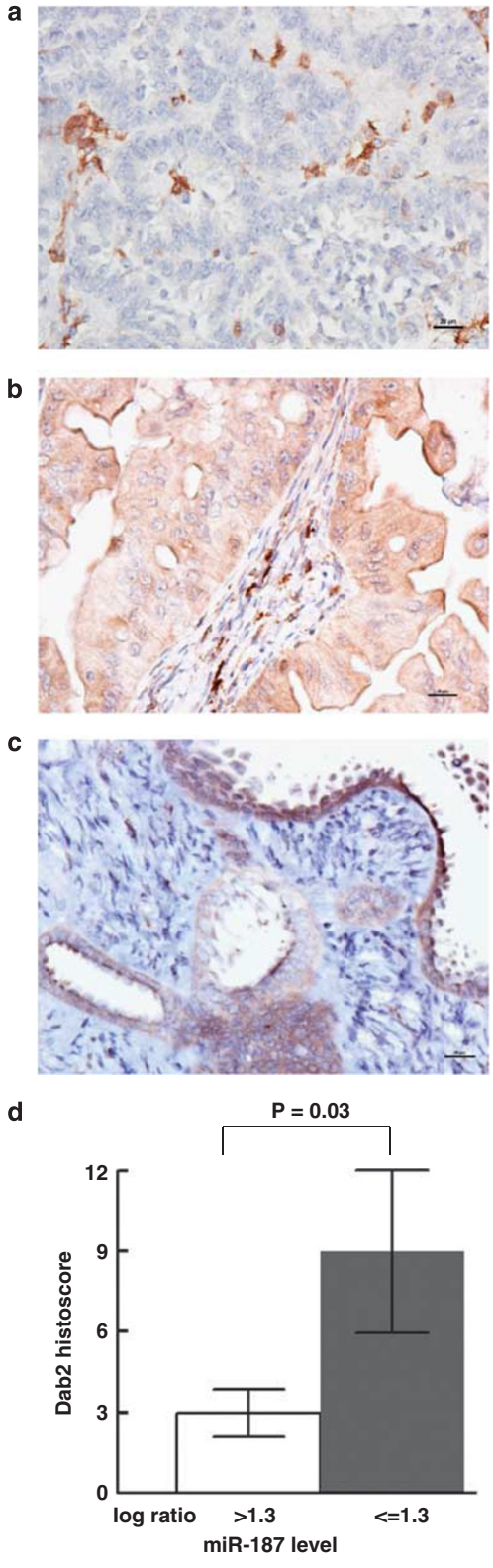

Discussion

This is the first time that miR-187 has been reported to be upregulated in human ovarian cancer (Table 1), although several miRNAs (miR-200a, miR-200b, miR-200c and miR-141) have been reported to be highly expressed in human ovarian cancer (Iorio *et al*., 2007). Although aberrant expression of various miRNAs is believed to have an important role in ovarian tumorigenesis (Iorio *et al*., 2007; Lu *et al*., 2007; Laios *et al*., 2008; Nam *et al*., 2008; Yang *et al*., 2008; Eitan *et al*., 2009; Hu *et al*., 2009), the relationships between miR-200 levels in the prognoses of ovarian cancer and patients have been conflicting (Nam *et al*., 2008; Hu *et al*., 2009). Higher expressions of miR-200 in ovarian serous carcinoma ($n=20$) are significantly correlated with poorer prognosis (Nam *et al*., 2008). On the contrary, Hu *et al*. (2009) reported that patients with advanced disease and higher miR-200a expression had better prognoses than those with lower miR-200a expression ($n=55$). Our study boasts the largest number of patients with ovarian cancer ever reported for miRNAs ($n=176$), allowing us to investigate paradoxical phenomena such as the high levels of miR-200a and miR-187 expression seen in ovarian cancer as opposed to benign ovarian tissues (Table 1 and Figure 1a), and how the very high expression levels of these two miRNAs are significantly associated with a better prognosis (Table 2 and Supplementary Table 2).

EMT is a critical step in tumor progression (Thiery, 2002). miR-200-family members are fundamental regulators of EMT (Gregory *et al*., 2008; Peter, 2009), whereas miR-30 (Braun *et al*., 2010) and miR-661 (Vetter *et al*., 2010) are also involved in this regulation. miR-200s directly suppress ZEB1 and ZEB2, which are repressors of E-cadherin. Upregulation of miR-200a

Figure 5 Reverse correlations between Dab2 and miR-187 levels in ovarian cancer. (**a**) There were no Dab2 immunoreactivities in serous ovarian cancer cells that expressed high levels of miR-187. In this section, histiocytes in adjacent stroma were stained positive for Dab2 (scattered brown cells), serving as internal positive controls. (**b**) Dab2 protein (light brown regions) was weakly stained in serous ovarian cancer cells with lower levels of miR-187 than those in panel **a**. (**c**) Epithelia of benign ovarian tumors with low levels of miR-187 expressed prominent levels of Dab2 protein (dark brown). (**d**) Dab2 immunoreactivities were analyzed by histoscores, which is the percentage of Dab2-positive cells multiplied by its staining intensity. Histoscores were analyzed in tissue slides derived from 176 patients with ovarian cancer, with grouping that was identical to that in Figure 1b. The histoscores of the low-miR-187-expression group (log ratio $\leqslant 1.3$, $n=73$) were significantly higher than those of the group with higher miR-187 expression (log ratio >1.3, $n=103$).

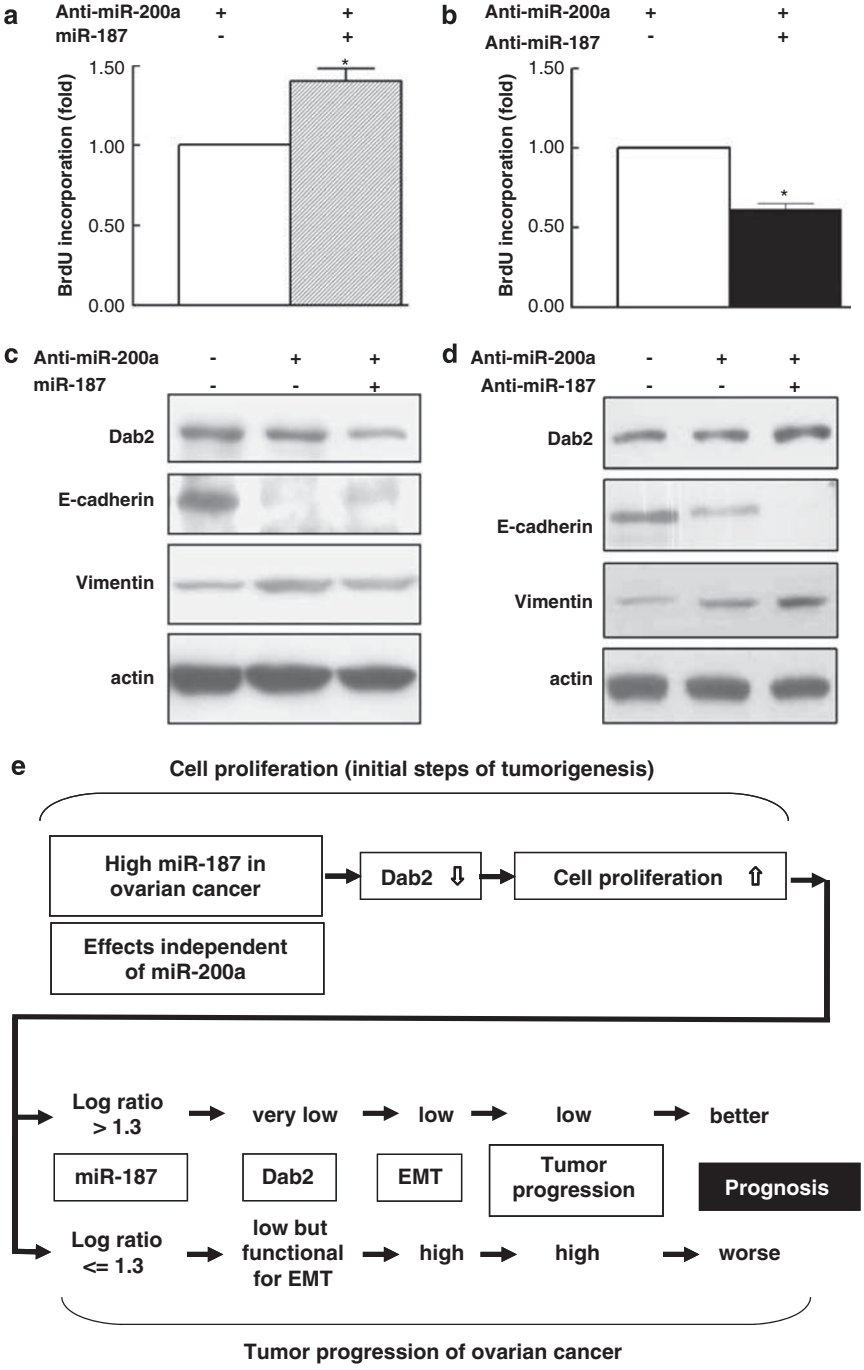

Figure 6 The dual roles played by miR-187 in ovarian cancer cells through fine tuning of Dab2 protein levels were independent of miR-200a. In miR-200a-knockdown SKOV3 cancer cells, overexpression of miR-187 inhibited Dab2 protein levels, increased cell proliferation (**a**) and inhibited EMT, which was shown by increased E-cadherin protein and decreased vimentin levels (**c**). In the same miR-200a-knockdown cancer cells, transfection with anti-miR-187 exerted the opposite effects of miR-187 (**b**, **d**). Actin was used to confirm equal protein inputs in all lanes. The quantitative results of immunoblots are summarized in Supplementary Figure 7. The data shown as mean ± s.e. are calculated from three independent experiments. $*P<0.05$ when compared with controls. (**e**) Expression of miR-187 is generally higher in ovarian cancer than in benign ovarian epithelia. Through inhibition of Dab2, which acts as a tumor suppressor, high levels of miR-187 promote cell proliferation (upper panel). During tumor cell evolution, some ovarian cancers continue upregulating miR-187 levels (shown here by the miR-187 $>$log ratio 1.3 group), resulting in very low protein levels of Dab2, low EMT and a better prognosis. On the other hand, some ovarian cancers stop upregulating miR-187 levels (shown here by the miR-187 $\leqslant$log ratio 1.3 group) and thus maintain low but functional levels of Dab2 that is required for EMT, resulting in aggressive tumor progression and a poorer prognosis (lower panel).

increases E-cadherin and inhibits cancer progression by suppressing EMT (Gregory *et al*., 2008). In agreement with those findings, we also found that very high expression of miR-200a is associated with a better prognosis (Supplementary Table 2), presumably through suppression of EMT. For the first time, very high levels of miR-187 in ovarian cancer patients are found to be associated with better survival (Table 2 and Figure 1b), possibly through regulation of Dab2-mediated EMT.

To support that miR-187 exerts dual Dab2-mediated roles in regulating the development of ovarian cancer, we first confirmed that miR-187 directly targets Dab2 (Figure 2) and stimulates the proliferation of ovarian cancer cells (Figure 3). Overexpression of miR-187 inhibits Dab2, vimentin, phospho-FAK and cell migration, and such inhibition can be rescued by re-expression of a T7-tagged Dab2 that cannot be suppressed by miR-187 (Figure 4). These results collectively confirm that miR-187 regulates EMT through Dab2.

miR-187 is located in chromosome 18q12.2, and its target motif is a 7mer8-m8 seed-matched site of position 77–83 of the Dab2 3′-UTR (Targetscan4.0, 2007). In clinical ovarian cancer tissues, reverse correlations between Dab2 immunoreactivities and miR-187 levels (Figure 5) also support the hypothesis that miR-187 targets Dab2. Dab2 is downregulated in several cancers and is frequently undetectable in breast and ovarian cancer (Mok *et al*., 1998; Fazili *et al*., 1999). In Dab2-knockout mice, Dab2-haplodeficient ($dab2^{+/-}$) female mice frequently develop widespread uterine hyperplasia and ovarian pre-cancer morphological features (Yang *et al*., 2006). Interestingly, Dab2 is also crucial for transforming growth factor-β-induced EMT, where downregulation of Dab2 prevents EMT and promotes apoptosis in murine mammary gland epithelial cells (Prunier and Howe, 2005). Dab2 may be a tumor suppressor, but in late cancer stages it is also functionally important for tumorigenesis by promotion of EMT-mediated metastasis (Prunier and Howe, 2005; Chaudhury *et al*., 2010). During the progression of human squamous cell carcinoma, downregulation of Dab2 switches transforming growth factor-β from tumor-suppressor to tumor-promoting functions (Hannigan *et al*., 2010). Clearly, Dab2 appears to have a dual role in tumor progression.

In conclusion, our study results demonstrate distinctly dual roles of miR-187, through Dab2 targeting, in cell proliferation and tumor progression (Figure 6). In the initial steps of tumorigenesis, upregulated miR-187 suppresses Dab2, promoting cell proliferation. During the microevolution of cancer cells, some cells further upregulate miR-187 and inhibit Dab2-dependent EMT, which is associated with tumor invasiveness. The overshooting mechanism may account for the paradoxical observation that ovarian cancers with high miR-187 levels were associated with better survival (Figure 1b and Table 2). On the other hand, in cancer cells that maintain the increased miR-187 levels low enough, the functional Dab2 promotes EMT, tumor progression and metastases, which are associated with poorer prognoses of cancer patients (Figure 6e). Of note, the above effects of miR-187 are independent of miR-200a (Figure 6).

Materials and methods

Cell culture

Seven ovarian cancer cell lines (SKOV3, OVCAR-3, TOV-21G, TOV112D, OV-90, MDAH2774 and CAOV3) were obtained from the American Type Culture Collection (Manassas, VA, USA). The ovarian cancer cell line BR was established as described previously (Wang *et al*., 1998). An immortalized human ovarian surface epithelial cell line (IOSE-80PC), originally from Dr Andrew K Godwin (Fox Chase Cancer Center, Philadelphia, PA, USA) (Yang *et al*., 2004), was provided by Dr Peter CK Leung (British Columbia Children's and Women's Hospital, Vancouver, BC, Canada) (Choi *et al*., 2006). Another human ovarian surface epithelial (HOSE) cell line was provided by Dr SW Tsao (University of Hong Kong, Hong Kong) (Chung *et al*., 2005). Cells were cultured in 10% fetal bovine serum, penicillin (100 U/ml), streptomycin (100 U/ml) and Dulbecco's modified Eagle's medium (DMEM)/F12 media at 37 °C in a 5% CO_2 atmosphere.

Patients and ovarian tumor tissues

Tissue samples (FFPE tumor blocks) were available from 176 patients with ovarian cancer. Clinical information of the patients was archived in the databank of the Division of Gynecologic Oncology, Chang Gung Memorial Hospital, Taiwan. Benign epithelial ovarian tumor tissues were used as controls. Additional 20 fresh frozen samples of ovarian cancer were included for confirmation of the correlation between miR and its targeted gene (Supplementary Table 3). This translational study was approved by the Institutional Review Board of the Chang Gung Memorial Hospital (IRB No. 95-1364B and 97-1444C).

RNA extraction

RNA was extracted from FFPE tissues by using the Recover All Total Nucleic Acid Isolation system (Ambion, Austin, TX, USA) as described previously (Chao *et al*., 2010). In brief, FFPE tissues were cut into 2–3 sections of 10-μm thickness. Tumor tissues were carefully macrodissected from section slides using a scalpel and transferred into a sterile 1.5-ml centrifuge tube. The paraffin was removed by using 100% xylene at 50 °C for 3 min. After centrifugation, xylene was discarded and the pellet was washed with 100% ethanol and air-dried. The pellet was protease-digested for 3 h at 50 °C and RNA was purified through filter cartridges. Total RNA was extracted from cell lines or fresh frozen tissues using TRIZOL (Invitrogen, Carlsbad, CA, USA).

Real-time qPCR miRNA assay of cell lines and ovarian tissues

miRNA profiling of human ovarian cancer cell lines and immortalized human ovarian surface epithelial cell lines was performed by using the TaqMan MicroRNA Assays Human Panel Early Access kit containing 157 mature miRNAs (Applied Biosystems, Foster City, CA, USA). The expression levels of miR-187 and miR-200a in both cell lines and FFPE tissues were analyzed by using the TaqMan MicroRNA Assay (#ABM000500; Applied Biosystems). The expression levels of hsa-miR-16 (TaqMan MicroRNA Assay, #ABM000008) were used as internal control. The expression levels of DAB2 in cell lines were quantified by using the SYBR green assay (Applied

Biosystems). The expression levels of glyceraldehyde-3-phosphate dehydrogenase (GAPDH) were used as internal control. The primer sequences for DAB2 were as follows: forward, 5′-GGGCATTTGGTTACGTGTG-3′ and reverse, 5′-CTTTGC TGGCTTCCTCTATC-3′. The primer sequences for ZEB1 were as follows: forward, 5′-AAGAATTCACAGTGGAGAG AAGCCA-3′ and reverse, 5′-CGTTTCTTGCAGTTTGGGC ATT-3′. For amplification of GAPDH, the primers used were as follows: forward, 5′-GGTATCGTGGAAGGACTCATG AC-3′ and reverse, 5′-ATGCCAGTGAGCTTCCCGT-3′. The amplification conditions were as follows: initial denaturation for 10 min at 95 °C, followed by 45 cycles of 95 °C for 15 s and 60 °C for 1 min. The reactions were performed by using the ABI PRISM 7900 HT instrument (Applied Biosystems). A mean cycle of threshold (C_t) value for each duplicate measurement was calculated.

Plasmids

The expression vector of the selected miR-187 and the scrambled control were constructed by annealing the following oligonucleotides: miR-187 forward (F): 5′-AGCTTGGTCGG GCTCACCATGACACAGTGTGAGACCTCGGGCTACAA CACAGGACCCGGGCGCTGCTCTGACCCCTCGTGTCT TGTGTTGCAGCCGGAGGGACGCAGGUCCGCAA-3′ and miR-187 reverse (R): 5′-TGCGGACCTGCGTCCCTCCGGC TGCAACACAAGACACGAGGGGTCAGAGCAGCGCCC GGGTCCTGTGTTGTAGCCCGAGGTCTCACACTGTGT CATGGTGAGCCCGACC-3′; scrambled forward: 5′-AGCT TGTGTAACACGTCTATACGCCCAGTGTAACACGTCT ATACGCCCAGAT-3′ and scrambled reverse: 5′-ATCTGGG CGTATAGACGTGTTACACTGGGCGTATAGACGTGT TACACA-3′, in DNA annealing buffer (30 mM HEPES (pH 7.4), 100 mM potassium acetate and 2 mM magnesium acetate). The mixture was heated at 95 °C for 5 min and then incubated at 37 °C for 1 h. The inserts were ligated into pcDNA3.1 (Invitrogen) treated with *Hin*dIII (miR-187) and *Hin*dIII/*Eco*RV (scrambled control), respectively. The pMir luciferase reporter vectors contained the 3′-UTR of the DAB2 gene (Luc-DAB2-3′-UTR) that were amplified from IOSE cDNA using the DAB2-3′-UTR forward primer 5′-CAAAGCTGATAGC CAGACACGTTC-3′ and the DAB2-3′-UTR reverse primer 5′-CCTGAGCATTAAGGGTCAAGAG-3′. The forward primer for mutant Luc-Dab2-3′-UTR was 5′-CAAAGCTGA TAGCCAGACAATTTC-3′. The pMir luciferase reporter vectors contained the 3′-UTR of the ZEB1 gene (Luc-ZEB1-3′-UTR) by using the ZEB1-3′-UTR forward primer 5′-CCA CTGACTCTGTCAGAGAAACTG-3′ and the ZEB1-3′-UTR reverse primer 5′-GCTTCCCTGAAATGACCTGA-3′. The PCR conditions were as follows: 95 °C for 5 min, followed by 40 cycles of 95 °C for 1 min, 55 °C for 1 min and 72 °C for 90 sec, and a final extension step at 72 °C for 10 min. After confirming the sequence, the PCR products were digested with Hin*d*III and ligated into the Hin*d*III/CIP-treated pMir-reporter vector (Ambion). The correct assembly of the constructs was confirmed by DNA sequencing. The Dab2 expression plasmid was a gift from Dr Ching-Ping Tseng (Department of Medical Biotechnology and Laboratory Science, Chang Gung University).

DNA transfection

For miR-187 overexpression experiments, pcDNA-miR-187 or pcDNA-scrambled were transfected into SKOV3 cells using Lipofectamine 2000 (Invitrogen) according to the manufacturer's protocol. Transient transfection was performed 48–72 h prior to cell harvest, unless otherwise specified. For anti-miR-187 experiments, the anti-miR-187 or anti-scrambled duplexes (Exiqon, Vedbaek, Denmark) were transfected into SKOV3 cells at a final concentration of 5 nM using the Lipofectamine RNAiMAX (Invitrogen) according to the manufacturer's instructions. Transient transfection was performed 72 h prior to cell harvest, unless otherwise specified.

The LNA-anti-miR-187 sequence was 5′-CCGGCTGCAA CACAAGACACGA-3′; the LNA-anti-miR-200a sequence was 5′-ACATCGTTACCAGACAGTGTTA-3′ and the LNA-anti-scramble sequence was 5′-GTGTAACACGTCTATACG CCCA-3′.

Luciferase reporter assay

Cells were transfected with DNA and the Lipofectamine 2000 reagent in OPTI-MEM medium. Lipofectamine 2000 and DNA were mixed gently and incubated at room temperature for 30 min to allow the formation of DNA–Lipofectamine 2000 complexes. The cells were placed in serum-free medium and then overlaid with DNA–liposome complexes. The cells were lysed with 1 × Reporter lysis buffer (Promega, Madison, WI, USA) and luciferase activity was measured by using the Dual-Glo Luciferase assay system (Promega) according to the manufacturer's protocol. In each sample, luciferase activity was normalized to *Renilla* luciferase activity to minimize inherent variation in transfection efficiency.

Western blot analysis

Cells were harvested, washed twice in phosphate-buffered saline (PBS) and lysed in ice-cold radio-immunoprecipitation assay lysis buffer (1% Triton X-100, 1% NP-40, 0.1% sodium dodecyl sulfate, 0.5% DOC, 20 mM Tris-hydroxymethyl-aminomethane (Tris–HCl, pH 7.4), 150 mM NaCl, protease inhibitor cocktail (Sigma, St Louis, MO, USA) and phosphatase inhibitor (Sigma)) for 30 min. The lysates were mixed with 4 × sample buffer, boiled and fractionated by sodium dodecyl sulfate–PAGE.

Following electrophoretic separation on 8% sodium dodecyl sulfate–PAGE gel, the proteins on the gels were transferred to nitrocellulose membranes (Amersham Pharmacia Biotech, Uppsala, Sweden). The blots were probed with an antibody specific to DAB2 (Becton Dickinson, Franklin Lakes, NJ, USA), phospho-397 FAK (Abcam, Cambridge, MA, USA), FAK (Cell Signaling Technology, Danvers, MA, USA), E-cadherin (Epitomics, Burlingame, CA, USA), vimentin (Epitomics) and appropriate secondary antibodies. The labeled bands were subsequently detected by enhanced chemiluminescence (ECL; Millipore, Bedford, MA, USA). For each sample, band intensities were normalized to β-actin (Sigma) (Chao *et al*., 2010).

BrdU incorporation assay

To study the effect of miR-187 on proliferation ability, SKOV3 cells that overexpressed either miR-187 or anti-miR-187 were seeded in a complete culture medium at a density of 10^4 cells per well in a 96-well plate for 12 h. After addition of BrdU, the cells were grown for another 12 h. DNA synthesis was assayed by ELISA for BrdU incorporation (Roche Applied Science, Indianapolis, IN, USA) (Chao *et al*., 2010).

Cell migration assays

SKOV3 cells (2×10^4/well) overexpressing either miR-187 or anti-miR-187 were plated in DMEM, 10% FBS in the upper chamber of 8-mm pore (24-well) transwells (Corning and Transwell, NY, USA). The lower chamber was filled with 800 μl of DMEM/F12 media containing 0.5 μg/ml fibronection (Sigma). After a 24-h incubation period, the cells that had

migrated through the pores and reattached to the lower chamber were fixed with methanol and stained with Giemsa (Sigma) and imaged, and the number of migrating cells was counted. Five random fields were analyzed for each chamber. The assays were conducted in three independent experiments.

Wound-closure assays
To study the effect of miR-187 on cell migration, SKOV3 cells that overexpressed either miR-187 or anti-miR-187 were analyzed by using the Culture-Inserts (Ibidi, Germany). The Culture-Inserts were transferred to 3.5-cm dishes and cells were seeded in a complete culture medium at a density of 4200/well in the Culture-Inserts. After 12 h of culture, the Culture-Inserts were removed to create cell-free gaps. The medium was replaced with fresh serum-free medium. Phase-contrast images of the gaps were captured at 0 h (control), and 16 h (miR-187) or 24 h (anti-miR-187) of incubation using an inverted microscope (magnification, $\times 10$). Wound-closure analyses were quantified by using the WimScratch software (Wimasis, Munich, Germany). The percentage of migrated cells was calculated by subtracting the cell coverage % of the remaining wound areas from the original % at the beginning of experiment. The result was then normalized by the control group.

Immunohistochemical study
FFPE tissue slices (ovarian cancer and normal ovary, each 4-μm thick) were deparaffinized in xylene and rehydrated in decreasing concentrations of ethanol. The sections were immunostained with an anti-DAB2 antibody (Santa Cruz Biotechnology, Santa Cruz, CA, USA) at 1:75 dilution by using the ES automated immunohistochemical stainer (Ventana Medical Systems, Tucson, AZ, USA), as described previously (Chao *et al*., 2006). The overall immunohistochemical score (histoscore) in this study was the percentage of positive cells multiplied by its staining intensity (0 = negative, 1 = weak, 2 = moderate, 3 = strong), and ranged from 0 to 300 (100% multiplied by 3) (Liao *et al*., 2011).

Confocal immunofluorescence microscopy
SKOV3 cells (2×10^5/well in six-well plates) were grown on sterilized coverslips overnight and the cells were co-transfected with either miR-187 and pCR3.1-EGFP or anti-miR-187 and pCR3.1-EGFP by using Lipofectamine 2000 (Invitrogen). After 48 h, the cells were fixed with 3.7% formaldehyde for 10 min prior to permeabilization with Triton X-100 (0.2% in PBS, for 5 min) and incubated in blocking buffer (5% normal goat serum in PBS) to reduce non-specific binding for 1 h at room temperature. The cells were incubated with a polyclonal anti-rabbit vimentin antibody (Epitomics; 1:50) for 1 h. After washing, the cells were incubated with an Alexa Fluor-546 anti-rabbit IgG (Invitrogen; 1:200) for 1 h prior to washing and mounting. The slides were mounted with the Vectashield mounting medium (Vector Laboratories, Burlingame, CA, USA) and analyzed by using the Leica TCS SP2 laser scanning confocal system (Leica Inc, Germany).

Microarray analysis and target prediction of miRNA-overexpressing ovarian cancer cell lines
Parallel analyses of gene expression profiles in ovarian cancer cell lines overexpressing miR-187 or cells expressing vector alone were performed by using the Human Genome U133A array (Affymetrix, Santa Clara, CA, USA), which contains the oligonucleotide probe set for 22 218 human genes (Tsai *et al*., 2007; Lee *et al*., 2009). We used TargetScan 4.0 (http://www.targetscan.org/) to identify potential target sites of differentially expressed miRNAs.

Bioinformatics and data analysis
The signal intensities of the miRNA data in ovarian cancer cell lines and immortalized human ovarian surface epithelia cell lines were normalized by the quantile normalization method combined with a permutation test by using BioInformatics Toolbox Software 3.1 (R2008a) in MATLAB. SAM (Significance Analysis of Microarrays) by using a software from the Stanford University labs (Tusher *et al*., 2001) was performed to investigate the differential expression of miRNAs.

In transfection experiments, Student's *t*-tests were used to evaluate the effects of miRNA or anti-miRNA on mRNA and targeted protein levels, which were analyzed by qPCR and western blot analyses, respectively. Two-tailed *P*-values <0.05 were considered significant.

The main outcome measures were recurrence-free survival and OS. Recurrence-free survival was defined as the time interval between the date of primary surgery and the date of the first recurrence. OS was calculated as the time period from the date of primary surgery to the date of death. A Cox proportional hazards regression model was used for the analysis of prognostic factors. The results were expressed as hazard ratios with 95% confidence intervals. To define the independent contribution of each risk factor (clinical variables and miRNA expression), we performed a multivariable Cox proportional hazards analysis. Survival curves were calculated by the Kaplan–Meier method and compared for statistical significance by using the log-rank test. Grouping cut-off points were selected as the value corresponding to the highest accuracy (sum of maximum sensitivity and specificity) of the receiver operating characteristics curve analysis. Patients were grouped into the low-miR-187 group (log ratio $\leqslant 1.3$, $n = 73$) and the high-miR-187 group (log ratio >1.3, $n = 103$). Statistical analyses of the clinical endpoints were performed by using the SPSS statistical software, version 17.0 (SPSS Inc, Chicago, IL, USA). Two-tailed *P*-values <0.05 were considered significant.

Conflict of interest

The authors declare no conflict of interest.

Acknowledgements

We thank Ching-Ling Wang, Jung-Erh Yang and Ying-Yu Lin for technical assistance; the Division of Gynecologic Oncology of Chang Gung Memorial Hospital for clinical data retrieval; Shih-Yee Mimi Wang (University of Illinois College of Medicine, Rockford) for language editing and Professor Ching-Ping Tseng (Chang Gung University) for discussion and advices. This study was supported by grants from the National Science Council (NSC99-2314-B-182A-087-MY3 to AC), the National Research Program for Genomic Medicine (NSC97-3112-B-001-020 to Y-SL), the Chang Gung Medical Foundation (CMRPG360953/4, 391451 to AC; IRB No. 95-1364B, 97-1444C, 99-2072C, 99-2411C) and the Department of Health (DOH99-TD-B-111-005 to C-HL; DOH99-TD-C-111-006 to AC and T-HW).

References

Bartel DP. (2004). MicroRNAs: genomics, biogenesis, mechanism, and function. *Cell* **116**: 281–297.

Bast Jr RC, Feeney M, Lazarus H, Nadler LM, Colvin RB, Knapp RC. (1981). Reactivity of a monoclonal antibody with human ovarian carcinoma. *J Clin Invest* **68**: 1331–1337.

Berek JS, Friedlander M, Hacker NF. (2010). Epithelial ovarian, fallopian tube, and peritoneal cancer. In: Berek JS, Hacker NF (eds). *Berek & Hacker's Gynecologic Oncology*. Lippincott Williams & Wilkins, pp 444–508.

Braun J, Hoang-Vu C, Dralle H, Huttelmaier S. (2010). Down-regulation of microRNAs directs the EMT and invasive potential of anaplastic thyroid carcinomas. *Oncogene* **29**: 4237–4244.

Chao A, Wang TH, Lee YS, Hsueh S, Chao AS, Chang TC *et al*. (2006). Molecular characterization of adenocarcinoma and squamous carcinoma of the uterine cervix using microarray analysis of gene expression. *Int J Cancer* **119**: 91–98.

Chao A, Tsai CL, Wei PC, Hsueh S, Chao AS, Wang CJ *et al*. (2010). Decreased expression of microRNA-199b increases protein levels of SET (protein phosphatase 2A inhibitor) in human choriocarcinoma. *Cancer Lett* **291**: 99–107.

Chaudhury A, Hussey GS, Ray PS, Jin G, Fox PL, Howe PH. (2010). TGF-beta-mediated phosphorylation of hnRNP E1 induces EMT via transcript-selective translational induction of Dab2 and ILEI. *Nat Cell Biol* **12**: 286–293.

Choi JH, Choi KC, Auersperg N, Leung PC. (2006). Differential regulation of two forms of gonadotropin-releasing hormone messenger ribonucleic acid by gonadotropins in human immortalized ovarian surface epithelium and ovarian cancer cells. *Endocr Relat Cancer* **13**: 641–651.

Chung CM, Man C, Jin Y, Jin C, Guan XY, Wang Q *et al*. (2005). Amplification and overexpression of aurora kinase A (AURKA) in immortalized human ovarian epithelial (HOSE) cells. *Mol Carcinog* **43**: 165–174.

Eitan R, Kushnir M, Lithwick-Yanai G, David MB, Hoshen M, Glezerman M *et al*. (2009). Tumor microRNA expression patterns associated with resistance to platinum based chemotherapy and survival in ovarian cancer patients. *Gynecol Oncol* **114**: 253–259.

Fazili Z, Sun W, Mittelstaedt S, Cohen C, Xu XX. (1999). Disabled-2 inactivation is an early step in ovarian tumorigenicity. *Oncogene* **18**: 3104–3113.

Gregory PA, Bert AG, Paterson EL, Barry SC, Tsykin A, Farshid G *et al*. (2008). The miR-200 family and miR-205 regulate epithelial to mesenchymal transition by targeting ZEB1 and SIP1. *Nat Cell Biol* **10**: 593–601.

Griffiths-Jones S. (2004). The microRNA registry. *Nucleic Acids Res* **32**: D109–D111.

Hannigan A, Smith P, Kalna G, Lo Nigro C, Orange C, O'Brien DI *et al*. (2010). Epigenetic downregulation of human disabled homolog 2 switches TGF-beta from a tumor suppressor to a tumor promoter. *J Clin Invest* **120**: 2842–2857.

Hu X, Macdonald DM, Huettner PC, Feng Z, El Naqa IM, Schwarz JK *et al*. (2009). A miR-200 microRNA cluster as prognostic marker in advanced ovarian cancer. *Gynecol Oncol* **114**: 457–464.

Iorio MV, Visone R, Di Leva G, Donati V, Petrocca F, Casalini P *et al*. (2007). MicroRNA signatures in human ovarian cancer. *Cancer Res* **67**: 8699–8707.

Jemal A, Siegel R, Ward E, Murray T, Xu J, Thun MJ. (2007). Cancer statistics, 2007. *CA Cancer J Clin* **57**: 43–66.

Laios A, O'Toole S, Flavin R, Martin C, Kelly L, Ring M *et al*. (2008). Potential role of miR-9 and miR-223 in recurrent ovarian cancer. *Mol Cancer* **7**: 35.

Lee YS, Chen CH, Tsai CN, Tsai CL, Chao A, Wang TH. (2009). Microarray labeling extension values: laboratory signatures for Affymetrix GeneChips. *Nucleic Acids Res* **37**: e61.

Liao CJ, Wu TI, Huang YH, Chang TC, Wang CS, Tsai MM *et al*. (2011). Overexpression of gelsolin in human cervical carcinoma and its clinicopathological significance. *Gynecol Oncol* **120**: 135–144.

Lu L, Katsaros D, de la Longrais IA, Sochirca O, Yu H. (2007). Hypermethylation of let-7a-3 in epithelial ovarian cancer is associated with low insulin-like growth factor-II expression and favorable prognosis. *Cancer Res* **67**: 10117–10122.

Metzler M, Wilda M, Busch K, Viehmann S, Borkhardt A. (2004). High expression of precursor microRNA-155/BIC RNA in children with Burkitt lymphoma. *Genes Chromosomes Cancer* **39**: 167–169.

Mok SC, Wong KK, Chan RK, Lau CC, Tsao SW, Knapp RC *et al*. (1994). Molecular cloning of differentially expressed genes in human epithelial ovarian cancer. *Gynecol Oncol* **52**: 247–252.

Mok SC, Chan WY, Wong KK, Cheung KK, Lau CC, Ng SW *et al*. (1998). DOC-2, a candidate tumor suppressor gene in human epithelial ovarian cancer. *Oncogene* **16**: 2381–2387.

Nam EJ, Yoon H, Kim SW, Kim H, Kim YT, Kim JH *et al*. (2008). MicroRNA expression profiles in serous ovarian carcinoma. *Clin Cancer Res* **14**: 2690–2695.

Peter ME. (2009). Let-7 and miR-200 microRNAs: guardians against pluripotency and cancer progression. *Cell Cycle* **8**: 843–852.

Prunier C, Howe PH. (2005). Disabled-2 (Dab2) is required for transforming growth factor beta-induced epithelial to mesenchymal transition (EMT). *J Biol Chem* **280**: 17540–17548.

Singh A, Settleman J. (2010). EMT, cancer stem cells and drug resistance: an emerging axis of evil in the war on cancer. *Oncogene* **29**: 4741–4751.

Takamizawa J, Konishi H, Yanagisawa K, Tomida S, Osada H, Endoh H *et al*. (2004). Reduced expression of the let-7 microRNAs in human lung cancers in association with shortened postoperative survival. *Cancer Res* **64**: 3753–3756.

Targetscan4.0 (2007). Prediction of microRNA targets. http://wwwtargetscanorg/cgi-bin/targetscan/vert_40/view_genecgi?taxid=9606&gs=DAB2&showcnc=0&shownc=0.

Thiery JP. (2002). Epithelial–mesenchymal transitions in tumour progression. *Nat Rev Cancer* **2**: 442–454.

Tsai MS, Hwang SM, Chen KD, Lee YS, Hsu LW, Chang YJ. *et al*. (2007). Functional network analysis of the transcriptomes of mesenchymal stem cells derived from amniotic fluid, amniotic membrane, cord blood, and bone marrow. *Stem Cells* **25**: 2511–2523.

Tusher VG, Tibshirani R, Chu G. (2001). Significance analysis of microarrays applied to the ionizing radiation response. *Proc Natl Acad Sci USA* **98**: 5116–5121.

Vetter G, Saumet A, Moes M, Vallar L, Le Bechec A, Laurini C *et al*. (2010). miR-661 expression in SNAI1-induced epithelial to mesenchymal transition contributes to breast cancer cell invasion by targeting Nectin-1 and StarD10 messengers. *Oncogene* **29**: 4436–4448.

Volinia S, Calin GA, Liu CG, Ambs S, Cimmino A, Petrocca F *et al*. (2006). A microRNA expression signature of human solid tumors defines cancer gene targets. *Proc Natl Acad Sci USA* **103**: 2257–2261.

Wang TH, Wang HS, Ichijo H, Giannakakou P, Foster JS, Fojo T *et al*. (1998). Microtubule-interfering agents activate c-Jun N-terminal kinase/stress-activated protein kinase through both Ras and apoptosis signal-regulating kinase pathways. *J Biol Chem* **273**: 4928–4936.

Yanaihara N, Caplen N, Bowman E, Seike M, Kumamoto K, Yi M *et al*. (2006). Unique microRNA molecular profiles in lung cancer diagnosis and prognosis. *Cancer Cell* **9**: 189–198.

Yang DH, Fazili Z, Smith ER, Cai KQ, Klein-Szanto A, Cohen C *et al*. (2006). Disabled-2 heterozygous mice are predisposed to endometrial and ovarian tumorigenesis and exhibit sex-biased embryonic lethality in a p53-null background. *Am J Pathol* **169**: 258–267.

Yang H, Kong W, He L, Zhao JJ, O'Donnell JD, Wang J *et al*. (2008). MicroRNA expression profiling in human ovarian cancer: miR-214 induces cell survival and cisplatin resistance by targeting PTEN. *Cancer Res* **68**: 425–433.

Yang WL, Godwin AK, Xu XX. (2004). Tumor necrosis factor-alpha-induced matrix proteolytic enzyme production and basement membrane remodeling by human ovarian surface epithelial cells: molecular basis linking ovulation and cancer risk. *Cancer Res* **64**: 1534–1540.

Supplementary Information accompanies the paper on the Oncogene website (http://www.nature.com/onc)